arXiv:1212.6759v2 [cond-mat.mes-hall] 6 Jan 2013

Interaction-Assisted Gap Opening in Moiré Graphene Superlattices

Justin C. W. Song[1,2], Andrey V. Shytov[3], and Leonid S. Levitov[1]
[1] *Department of Physics, Massachusetts Institute of Technology, Cambridge, Massachusetts 02139, USA*
[2] *School of Engineering and Applied Sciences, Harvard University, Cambridge, Massachusetts 02138, USA and*
[3] *School of Physics, University of Exeter, Stocker Road, Exeter EX4 4QL, U.K.*

We show that coupling of Dirac particles in graphene to moiré superlattice potential in G/hBN heterostructures is strongly affected by interactions. Interacting Dirac particles respond strongly to a pseudospin-dependent ('colored') potential arising due to the A-B sublattice modulation and relatively more weakly to a scalar potential which is sublattice-blind. As a result, the effective potential seen by electrons in graphene becomes predominantly 'colored,' leading to pseudospin-dependent Bragg scattering. Many-body effects generate giant enhancement of the gap at the Dirac point, which can overtake the enhancement of the minigaps opened by Bragg scattering at the superlattice Brillouin zone edges. We predict a power-law dependence for the gap vs. moiré pattern wavelength, which can be used to directly test the effects of interactions in experiment.

Electronic states in heterostructures comprised of graphene and hexagonal boron nitride (hBN) have interesting and potentially useful properties[1–3]. Both materials have hexagonal lattice structures with near-pefectly matched periods. Placing graphene on hBN, which is a wide-bandgap electric insulator, yields structures with low disorder, high carrier mobility, and improved device performance. A small period mismatch ($\approx 1.8\%$) of graphene and hBN leads to moiré superlattices with spatial periods reaching $\lambda_0 \approx 14\,\mathrm{nm}$ for perfectly aligned crystals. The electronic states in graphene have comparable deBroglie wavelength and are fully exposed to the hBN superlattice potental. A number of interesting phenomena were predicted in this system: Bloch minibands and changes in Fermi surface topology[4–6], replica Dirac points[7], and most recently, Hofstadter-type commensurability effects in magnetic field[8, 9], all successfully described by a noninteracting Dirac-Bloch model.

As we argue below, the noninteracting single-particle Dirac-Bloch picture, despite all the appeal it may have, is not fully adequate. We will see that this picture misses some important physics occurring near the Dirac point, which results from electron-electron interactions. Specifically, as we will discuss in detail below, interacting Dirac particles respond in a very different way to a scalar external potential which is sublattice-blind and a pseudospin-dependent ('colored') potential arising due to the A-B sublattice modulation. In the first case, interactions generate polarization that screens the potential. In the second case, interactions generate sublattice correlations that amplify the potential.

The interaction-induced amplification of colored potential leads to pseudospin-dependent Bragg scattering which has dramatic consequences for electronic states. First, a gap at the Dirac point opens up. Second, because Dirac mass term is a relevant perturbation in the renormalization group (RG) sense, this gap undergoes giant interaction-induced enhancement. Counter-intuitively, this enhancement can be much greater than the enhancement of the side gaps opened by Bragg scattering at principal superlattice harmonics, see Fig.1.

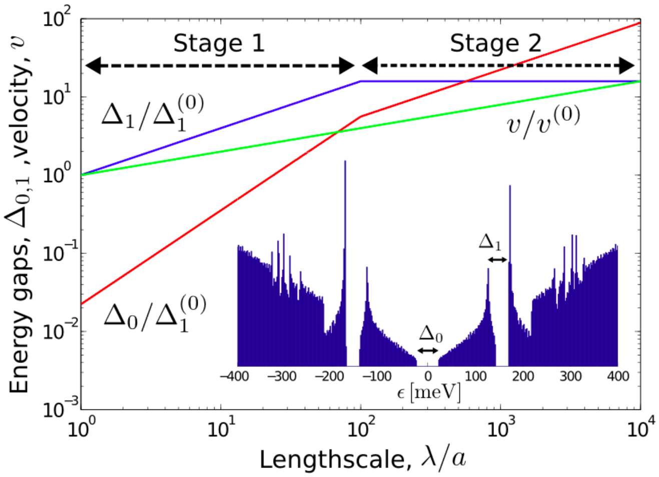

FIG. 1: Interaction-induced enhancement of couplings to the moiré superlattice potential. RG flow is shown for the gap at the Dirac point, Δ_0, and the gap opened by Bragg scattering at the principal superlattice harmonics, Δ_1 (red and blue lines). Renormalization proceeds in two stages described in the text: $a < \lambda < \lambda_0$ (stage 1) and $\lambda > \lambda_0$ (stage 2), where $a = 1.42\mathring{A}$ is carbon spacing, λ_0 is the moiré superlattice wavelength. Both gaps are enhanced from the noninteracting values $\Delta_0^{(0)}$, $\Delta_1^{(0)}$, however the gap Δ_0 undergoes a much larger enhancement and, despite a small initial value, eventually overtakes Δ_1. Both Δ_0 and Δ_1 grow faster than the carrier velocity v (green line). Inset shows the density of states near the Dirac point with the gap Δ_1 opened at the superlattice Bragg energy $\epsilon_0 = \frac{1}{2}\hbar v|\mathbf{b}|$, $|\mathbf{b}| = 2\pi/\lambda_0$. Parameters used: superlattice period $\lambda_0 = 14\,\mathrm{nm}$, scaling exponents $\beta = 0.6$, $\beta_v = 0.3$, initial values $\Delta_0^{(0)} \approx 0.02\Delta_1^{(0)}$ (see text).

Due to spatial oscillations of the coupling to moiré superlattice, the RG flow for these couplings proceeds in two separate stages: stage 1 describing renormalization at lengthscales up to the moiré wavelength, $\lambda < \lambda_0$, and stage 2 describing lengthscales $\lambda > \lambda_0$. The lengthscale at which RG terminates is controlled by the screening length which is set by the distance to the gates when those are metallic, as in Ref.[1], or by the screening length in the gate if the latter is realized by a proximal graphene layer, as in Ref.[13]. We find that stage 1 acts as a 'booster,' generating an enhancement of energy gaps which is much greater than that of carrier velocity. At stage 2 the growth of the side gap Δ_1 stalls whereas the gap Δ_0 continues to grow. As illustrated in Fig.1, the gap Δ_0 eventually can overtake Δ_1 even if the latter starts with a larger microscopic bare value.

Interaction-assisted enhancement of spectral gaps generated by microscopic interactions was proposed for a variety of different systems, e.g. for chiral metallic nanotubes[10] and for Quantum Spin-Hall effect in graphene where a gap is opened by spin-orbit coupling[11]. In Ref.[12], renormalization of a gap opened by sublattice modulation was analyzed using $1/N$ expansion, and a scaling exponent $\beta = 16/\pi^2 N$ was found. Our results for Δ_0 enhancement are consistent with Ref.[12] for $\lambda > \lambda_0$, however we find a much stronger enhancement at short lengthscales, $\lambda < \lambda_0$, where rapid RG growth occurs. This is so because the gap Δ_0 depends on a combination of microscopic parameters which renormalize independently, see Eq.(4), leading to a much steeper growth on stage 1 than on stage 2.

Besides establishing the hierarchy of energy scales for different gaps, our approach may help to shed new light on the recently observed insulating state, which arises despite the extreme cleanness of G/hBN systems[13, 14]. This state is observed at charge neutrality (CN) when the long-range disorder due to charge puddles is screened by gates. These observations, which are not understood, are particularly suprising because previous measurements have reported record-high mobilities in this system away from CN. Several scenarios are at the table: Ref.[13] attributes the resistive behavior at CN to weak localization due to remnant short-range disorder, a picture supported by a 'disorder by order' model [15]. Ref.[14] observes a highly resistive state, with strong insulating behavior turning on abruptly as a function of doping through CN and no appreciable sign of weak localization away from CN. This suggests an energy gap opening as a source of the insulating behavior. Indeed, as pointed out in Ref.[16], a gap at the Dirac point may be induced by sublattice modulation in hBN substrate. Yet without a sizeable boost by interaction effects the gap would be too small to explain the observations. Ref.[14], while leaning towards transport gap explanation, did not reach a definite conclusion about the origin of the observed behavior. Presently it is not known which of the two scenarios, a bandgap or a transport gap, is responsible for the new resistive state.

Turning to the analysis, since moiré superlattice period is much larger than the lattice constant, $\lambda_0 \gg a$, states in valleys K and K' are effectively decoupled. Hence we can describe each valley by an effective continuum Hamiltonian having a nontrivial pseudospin structure reflecting A-B sublattice modulation, and an oscillatory position dependence reflecting the superlattice periodicity:

$$H_0 = \begin{pmatrix} u_{11} f(\mathbf{x}) & v p_- + u_{12} f(\mathbf{x}) \\ v p_+ + u_{21} f(\mathbf{x}) & u_{22} f(\mathbf{x}) \end{pmatrix}, \qquad (1)$$

$$f(\mathbf{x}) = 2 \sum_{s=1,2,3} \cos(\mathbf{b}_s \mathbf{x} + \phi_s), \qquad (2)$$

$p_\pm = p_x \pm i p_y$. Here $\mathbf{b}_s$ ($s = 1, 2, 3$) are three Bravais vectors of the triangular superlattice oriented at 60^o angles relative to each other. Introducing pseudospin Pauli matrices $\sigma_{1,2,3}$ and adding long-range interactions we write

$$\mathcal{H} = \int d^2x \sum_{i=1}^{N} \psi_i^\dagger(\mathbf{x}) \left[v\sigma\mathbf{p} + m_3(\mathbf{x})\sigma_3 + m_0(\mathbf{x}) \right] \psi_i(\mathbf{x})$$
$$+ \frac{1}{2} \int d^2x \int d^2x' \frac{e^2}{\kappa|\mathbf{x} - \mathbf{x}'|} n(\mathbf{x}) n(\mathbf{x}'), \qquad (3)$$

where $m_3 = \frac{1}{2}(u_{11} - u_{22}) f(\mathbf{x})$, $m_0 = \frac{1}{2}(u_{11} + u_{22}) f(\mathbf{x})$. Here $N = 4$ is the number of spin/valley flavors, and $n(\mathbf{x}) = \sum_{i=1...N} \psi_i^\dagger(\mathbf{x}) \psi_i(\mathbf{x})$ is particle density. The off-diagonal terms u_{12} and u_{21}, which describe a gauge-field coupling generated by strain, can be incorporated in the $v\sigma\mathbf{p}$ term. However, *ab initio* studies[17] indicate that it is a small contribution compared to u_{11} and u_{22}.

The amplitude of sublattice modulation can be inferred from *ab initio* calculations[18] predicting $6(u_{11} - u_{22}) \approx 53\,\mathrm{meV}$ for the equal-period case, $\mathbf{b} = 0$. This gives amplitudes m_3 of individual Bragg harmonics which are more than 20 times smaller than the kinetic energy at the Bragg vector, $\epsilon_0 = \frac{1}{2}\hbar v|\mathbf{b}| \approx 150\,\mathrm{meV}$ estimated for largest superlattice period $\lambda_0 = 14\,\mathrm{nm}$ [19]. Hence we can employ perturbation theory in a small ratio m_3/ϵ_0.

The RG analysis of this Hamiltonian predicts that the m_3 harmonics grow under RG, whereas the m_0 harmonics do not grow (see below). Therefore, even if the microcopic values $m_3^{(0)}$ and $m_0^{(0)}$ are comparable, the bandgaps will be dominated by the m_3 harmonics. We can therefore estimate the bandgap opening at the edge of the superlattice Brillouin zone as $\Delta_1 = 2m_3$.

In addition, importantly, the interaction with superlattice leads to gap opening at the Dirac point. While a single m_3 harmonic is sign-changing, $\langle e^{i\mathbf{b}\mathbf{x}} \rangle = 0$, and thus it cannot give rise to such a gap by itself, a combination of three different harmonics can open up a gap at the Dirac point. Choosing triplets of harmonics with the sum of their wave-vectors adding up to zero, $\mathbf{b}_i + \mathbf{b}_j + \mathbf{b}_k = 0$, third-order perturbation theory in m_3 yields a constant sublattice-asymmetric term[26]

$$H_0' = \sum_{\pm\mathbf{b}_i, \pm\mathbf{b}_k} m_3\sigma_3 \frac{1}{v\sigma\mathbf{b}_i} m_3\sigma_3 \frac{1}{v\sigma\mathbf{b}_k} m_3\sigma_3 = -\frac{1}{2}\Delta_0\sigma_3, \qquad (4)$$

where $\Delta_0 = 12 m_3^3/(v|\mathbf{b}|)^2$ (the corresponding self-energy is shown in Fig.2a). Contributions similar to H_0' can also arise when two out of three $m_3\sigma_3$ terms are replaced

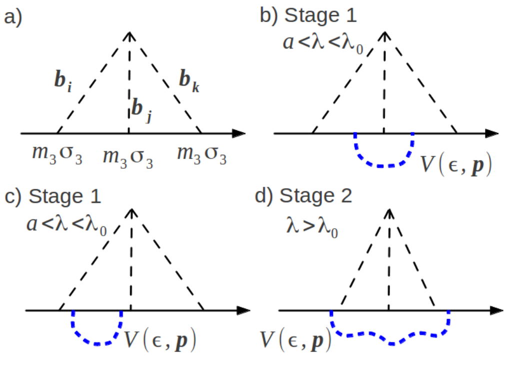

FIG. 2: Self-energy describing gap opening at the Dirac point (a) and log-divergent diagrams contributing to gap renormalization at one loop (b,c,d). The contributions (b) and (c), accounting for vertex renormalization and velocity renormalization, arise from integration over $|\mathbf{b}| < |\mathbf{p}| < p_0$ (stage 1), giving Eq.(10). The contribution (d) arises from $|\mathbf{p}| < |\mathbf{b}|$ (stage 2), giving Eq.(11).

by m_0 harmonics. However, since these harmonics do not grow under RG (see below), these contributions are small. Since $m_3 \ll \epsilon_0$, the predicted numerical value is small, $\Delta_0 \ll \Delta_1$ (similar observation was made in Ref.[20]). However, as we find shortly, the gap Δ_0 undergoes a giant boost due to interaction effects, growing faster than Δ_1. As a result, the physical values Δ_0 and Δ_1 become comparable.

The effects of interactions can be treated by an RG approach, constructed by extending the framework developed in Refs.[21–23] to account for renormalization of the terms m_0 and m_3 in Eq.(3). There are two distinct flavors of RG, a weak-coupling approach using $e^2/\hbar v \ll 1$ as an expansion parameter, and a large-N approach, both leading to qualitatively similar results[24]. We present detailed results for the large-N approach.

We first analyze renormalization of the m_0 and m_3 terms in Eq.(3) treating them as spatially uniform, ignoring the $\mathbf{x}$-dependence. The approach is valid over the range of lengthscales $a < \lambda \lesssim \lambda_0$. Larger lengthscales, $\lambda \gtrsim \lambda_0$, will be analyzed below. Renormalization is found by dressing the m_0 and m_3 vertices in Feynman diagrams with vertex corrections and analyzing the corresponding log-divergent contributions. The vertex correction for the m_0 term is cancelled by a corresponding contribution to the Greens function residue, owing to the Ward identity that follows from gauge invariance. This can be seen more explicitly by analyzing the self-energy

$$\Sigma(\epsilon,\mathbf{p}) = -\int \frac{d\epsilon' d^2p'}{(2\pi)^3} V(\epsilon',\mathbf{p}')G(\epsilon-\epsilon',\mathbf{p}-\mathbf{p}') \qquad (5)$$

with $G(\epsilon,\mathbf{p}) = 1/(i\epsilon - v\sigma\mathbf{p} - m_3\sigma_3 - m_0)$ the Greens function, and V representing the RPA interaction,

$$V(\epsilon,\mathbf{p}) = \frac{V_0(\mathbf{p})}{1 - NV_0(\mathbf{p})\Pi(\epsilon,\mathbf{p})}, \quad V_0(\mathbf{p}) = \frac{2\pi e^2}{\kappa|\mathbf{p}|}. \qquad (6)$$

Renormalization of the m_0 coupling, at linear order in m_0, is described by the quantity $\partial_{i\epsilon}\Sigma + \partial_{m_0}\Sigma$ which vanishes due to the form of $G(\epsilon,\mathbf{p})$.

We note that the cancellation of log-divergent contributions due to Ward identity does not apply to reducible diagrams. The latter generate a vertex correction given by the RPA dielectric constant $\epsilon = 1 - NV_0(\mathbf{p})\Pi(\epsilon,\mathbf{p})$, which describes intrinsic screening of m_0 vertex by inter-band and intra-band polarization.

Since m_3 vertex is distinct from m_0 vertex, we expect that log-divergent contributions do not cancel. As a result, electrons become ‘colored,’ i.e. their coupling to moiré superlattice potential is dominated by pseudospin-dependent interactions. Renormalization of m_3 was analyzed in Ref.[12] giving scaling exponent $\beta = 16/\pi^2 N$ which is two times larger than the value $\beta_v = 8/\pi^2 N$ found for velocity renormalization in Ref.[23]. This leads to RG flow equations for the m_3 coupling and velocity:

$$\frac{dm_3}{d\xi} = \beta m_3, \quad \frac{dv}{d\xi} = \beta_v v, \quad \frac{2\pi}{\lambda_0} < |\mathbf{p}| < p_0, \qquad (7)$$

where $\xi = \ln\frac{p_0}{|\mathbf{p}|}$ is the RG time parameter, with $p_0 \sim 2\pi/a$ the UV cutoff. Interestingly, the relation $\beta = 2\beta_v$ also holds in the weak-coupling approach. The RG flow, Eq.(7), predicts power-law enhancement to the m_3 harmonic and velocity for $a < \lambda < \lambda_0$:

$$m_3 = \left(\lambda/a\right)^{\beta} m_3^{(0)}, \quad v = \left(\lambda/a\right)^{\beta_v} v^{(0)}. \qquad (8)$$

Similarly, renormalization of $\Delta_0 \propto m_3^3/v^2$ is obtained by adding the contributions shown in Fig.2(b,c):

$$\begin{aligned} &\frac{\partial\Sigma}{i\partial\epsilon} + \frac{3\delta\Sigma}{\delta(\sigma_3 m_3)} - \frac{2\delta\Sigma}{\delta(v\sigma\mathbf{p})} = \int\frac{d\epsilon' d^2p'}{(2\pi)^3}\left[\frac{V(\epsilon',\mathbf{p}')}{(i\epsilon' - v\sigma\mathbf{p}')^2}\right. \\ &\left. - \frac{3V(\epsilon',\mathbf{p}')}{(i\epsilon' - v\sigma\mathbf{p}')(i\epsilon' + v\sigma\mathbf{p}')} - \frac{2V(\epsilon',\mathbf{p}')\epsilon'^2}{(i\epsilon' - v\sigma\mathbf{p}')^2(i\epsilon' + v\sigma\mathbf{p}')^2}\right] \\ &\approx (3\beta - 2\beta_v)\ln\frac{p_0}{|\mathbf{p}|}, \end{aligned} \qquad (9)$$

where we integrate over $|\mathbf{p}| \le p' \le p_0$. Taking N to be large, we find the value $32/\pi^2 N$ which is two times larger than the exponent β found in Ref.[12] and four times larger than the exponent β_v. As a result, Δ_0 grows under RG much faster than Δ_1:

$$\Delta_0 = \frac{12 m_3^3}{v^2|\mathbf{b}|^2} = \left(\lambda/a\right)^{3\beta - 2\beta_v}\Delta_0^{(0)}. \qquad (10)$$

A ten-fold increase in Δ_1 transaltes into a hundred-fold increase in Δ_0, see Fig.1. Thus, despite a handicap due to a small initial value, Eq.(4), the physical values for Δ_0 and Δ_1 are in the same ballpark.

For the sake of generality, and acknowledging an approximate character of the scaling dimensions obtained from one-loop RG, we shall leave β and β_v unspecified in the analytic expressions. An attempt to experimentally determine scaling exponents was made recently in

Ref.[25], where a systematic change of the period of quantum oscillations with carrier density was interpreted in terms of Fermi velocity renormalization, giving a value $\beta_v = 0.5$-0.55. This value is considerably larger than the one-loop RG result, $\beta_v = \frac{8}{\pi^2 N} \approx 0.2$. This discrepancy is not yet understood. For the plots in Fig.1 we used conservative values $\beta_v = 0.3$, $\beta = 2\beta_v = 0.6$.

At lengthscales larger than λ_0 renormalization is suppressed by spatial oscillations in the m_3 term. In this regime m_3 stops flowing and the gap Δ_1 stays constant, as shown by the horizontal line in Fig.1 (stage 2). In contrast, because the effective Hamiltonian H_0' is $\mathbf{x}$-independent, modes with $|\mathbf{p}| < \frac{2\pi}{\lambda_0}$ continue to provide an enhancement to the gap at the Dirac point, giving

$$\Delta_0(\lambda > \lambda_0) = (\lambda/\lambda_0)^{\beta}\,\Delta_0(\lambda_0). \tag{11}$$

The RG flow of Δ_0 at stage 2 is described by scaling exponent β which is smaller than the value $3\beta - 2\beta_v$ found for stage 1. Nevertheless, the growth of Δ_0 at stage 2 is still faster than that of velocity. As illustrated in Fig.1, Δ_0 can grow by several orders of magnitude, reaching Δ_1 for large enough λ. For the parameters chosen in Fig.1, Δ_0 (red line) overtakes Δ_1 (blue line), eventually making the gap at the Dirac point the largest gap in the system.

Renormalization of all the parameters in the system, including velocity v and the gap Δ_0, terminates either at an effective screening length set by proximal gate or at a lengthscale generated self-consistently through a gap opening at the Dirac point. In the first case, the effective screening length is determined by the distance to the gate or by the screening length for the gate, whichever is larger. In the second case, realized for systems with remote gates or when the screening length is very large, RG terminates at a self-consistently defined lengthscale controlled by the gap opened at the Dirac point,

$$\lambda_* = 2\pi/q_*, \quad \hbar q_* = \Delta_0(\lambda_*)/v(\lambda_*), \tag{12}$$

where the λ dependence is obtained from RG flow. A similar approach was employed in Ref.[10] to estimate interaction-enhanced gaps opened at the Dirac point in chiral metallic carbon nanotubes. Under realistic conditions, as discussed above, we expect $\Delta_0 \ll \epsilon_0 = \frac{1}{2}\hbar v|\mathbf{b}|$. Hence the selfconsistent lengthscale satisfies $\lambda_* \gg \lambda_0$. In this case, plugging the dependence from Eqs.(8),(11), we find $(\lambda_*/\lambda_0)^{1+\beta-\beta_v} = hv(\lambda_0)/[\lambda_0\Delta_0(\lambda_0)]$, giving

$$\Delta_0(\lambda_*) = \left(\frac{hv(\lambda_0)}{\lambda_0\Delta_0(\lambda_0)}\right)^{\frac{\beta}{1+\beta-\beta_v}} \Delta_0(\lambda_0) \propto \left(\frac{\lambda_0}{a}\right)^{\gamma}, \tag{13}$$

$\gamma = 3\beta - 2\beta_v - \frac{\beta(1+3\beta-3\beta_v)}{1+\beta-\beta_v}$. The predicted power-law dependence Δ_0 vs. moiré wavelength λ_0, Eq.(13), can be used to directly probe the effects of interactions. Setting $\beta = 2\beta_v$ (see discussion above), the expression for scaling exponent simplifies as:

$$\gamma = 4\beta_v - \frac{2\beta_v(1+3\beta_v)}{1+\beta_v} = \frac{\beta(2-\beta)}{2+\beta} \tag{14}$$

for which our one-loop RG gives $\beta = \frac{16}{\pi^2 N}$, $\gamma \approx 0.27$.

The predicted scaling $\Delta_0 \propto (\lambda_0/a)^{\gamma}$ can be tested by comparing the gap values measured in G/hBN systems with different misalignment angles, similar to how it was done in Ref.[19] for replica Dirac peaks. It is beneficial to be in the regime of small misalignment angles, since in this case the scatter in microscopic parameters determining bare $\Delta_0^{(0)}$ values is minimal, and at the same time the ratio λ_0/a is largest, which maximizes renormalization effects. This is the case for structures with near-perfect crystal axes alignment, such as those used in Ref.[9].

In summary, we predict that interactions have dramatic effect on the electronic properties of G/hBN systems. The bandgaps opened up by coupling to substrate are strongly enhanced by interactions. The predicted physical gap values can be many times greater than the bare gaps opened due to hBN sublattice modulation. The effect is most dramatic for the gap at the Dirac point which undergoes a giant enhancement that boosts it to a value comparable to or exceeding that for principal Bragg harmonics. These effects can be directly probed by measuring gap values for systems with different superlattice wavelengths, predicted to obey a power-law scaling $\Delta_0 \propto \lambda_0^{\gamma}$. It can also be probed by doping the system, since the gap enhancement due to screened interactions is considerably smaller than that in undoped system where interactions are unscreened. This leads to the gap collapsing upon doping, resulting in an enhancement in compressibility when the system is doped slightly above the gap. The strong effect on compressibility makes the interaction physics easily detectable in experiment.

We thank D. Golhaber-Gordon, A. Geim, P. Jarillo-Herrero, J. Williams and A. Young for useful discussions.

---

[1] C. R. Dean, et al. Nature Nanotech. **5**, 722 (2010).

[2] J. M. Xue et al., Nature Mater. **10**, 282 (2011).

[3] R. Decker et al., Nano Lett. **11**, 2291 (2011).

[4] F. Guinea, T. Low, Phil. Trans. R. Soc. A **368**, 5391 (2010).

[5] M. Barbier, P. Vasilopoulos, F. M. Peeters, Phys. Rev. B **81**, 075438 (2010).

[6] P. Burset, A. L. Yeyati, L. Brey, H. A. Fertig, Phys. Rev. B **83**, 195434 (2011).

[7] C. H. Park, L. Yang, Y. W. Son, M. L. Cohen, S. G. Louie, Nature Phys. **4**, 213 (2008); Phys. Rev. Lett. **101**, 126804 (2008).

[8] C. R. Dean, et al. arXiv:1212.4783

[9] L. A. Ponomarenko, et al. arXiv:1212.5012

[10] L. S. Levitov and A. M. Tsvelik, Phys. Rev. Lett. **90**, 016401 (2003).

[11] C. Kane, E. Mele, Phys. Rev. Lett. **95**, 226801 (2005).

[12] V. N. Kotov, B. Uchoa, and A. H. Castro Neto, Phys. Rev. B 80, 165424 (2009)

[13] L. A. Ponomarenko, et al. Nature Phys. **7**, 958-961(2011).

[14] F. Amet, J. R. Williams, K. Watanabe, T. Taniguchi, D.

Goldhaber-Gordon, arXiv:1209.6364

[15] S. Das Sarma, E. H. Hwang, and Q. Li, arXiv:1109.0988

[16] M. Kindermann, B. Uchoa and D. L. Miller , Phys. Rev. B **86**, 115415 (2012); arXiv:1205.3194

[17] B. Sachs, T. O. Wehling, M. I. Katsnelson, and A. I. Lichtenstein, Phys. Rev. B **84**, 195414 (2011).

[18] G. Giovannetti, P. A. Khomyakov, G. Brocks, P. J. Kelly, and J. van den Brink, Phys. Rev. B **76**, 073103 (2007).

[19] M. Yankowitz, et al., Nature Phys. **8**, 382 (2012).

[20] J. R. Wallbank, A. A. Patel, M. Mucha-Kruczynski, A. K. Geim, V. I. Fal'ko, arXiv:1211.4711

[21] J. González, F. Guinea, and M. A. H. Vozmediano, Nucl. Phys. B **424**, 595 (1994); Phys. Rev. B **59**, R2474 (1999).

[22] O. Vafek, Phys. Rev. Lett. **98**, 216401 (2007).

[23] D. T. Son, Phys. Rev. B **75**, 235423 (2007).

[24] V. N. Kotov, B. Uchoa, V. M. Pereira, F. Guinea, and A. H. Castro Neto, Rev. Mod. Phys. **84** 1067 (2012).

[25] D. C. Elias, et al. Nature Phys. **7**, 701 (2011).

[26] In Eq.(4) we have assumed $\delta\phi = \phi_1 + \phi_2 + \phi_3 = 0$. For nonzero $\delta\phi$ we find the dependence $\Delta_0(\delta\phi) = \cos(\delta\phi)\Delta_0$.